



Published in final edited form as:

Circ Arrhythm Electrophysiol. 2013 August ; 6(4): . doi:10.1161/CIRCEP.113.000448.

Electrical Homogenization of Ventricular Scar by Application of Collagenase: A Novel Strategy for Arrhythmia Therapy

Daigo Yagishita, MD¹, Olujimi A. Ajjola, MD, PhD¹, Marmar Vaseghi, MD, MS¹, Ali Nsair, MD², Wei Zhou, PhD³, Kentaro Yamakawa, MD³, Roderick Tung, MD¹, Aman Mahajan, MD, PhD^{1,3}, and Kalyanam Shivkumar, MD, PhD¹

¹UCLA Cardiac Arrhythmia Center, University of California, Los Angeles, CA

²Eli & Edythe Broad Center for Regenerative Medicine and Stem Cell Research, University of California, Los Angeles, CA

³Dept of Cardiac Anesthesia, University of California, Los Angeles, CA

Abstract

Background—Radiofrequency ablation for ventricular tachycardia (VT) is an established therapy. Use of chemical agents for scar homogenization represents an alternative approach. The purpose of this study was to characterize the efficacy of collagenase (CLG) application on epicardial ventricular scar homogenization.

Methods and Results—Myocardial infarcts were created in Yorkshire pigs (n=6) by intracoronary microsphere injection. After 46.6±4.3 days, CLG type 2, type 4, and purified CLG were applied in vitro (n=1) to myocardial tissue blocks containing normal myocardium, border-zone (BZ) and dense scar (DS). Histopathological studies were performed to identify the optimal CLG subtype. In-vivo high-density electroanatomic mapping of the epicardium was also performed, and BZ and DS surface area, and LPs were quantified before and after CLG-4 application (n=5). Of the CLG subtypes tested in vitro, CLG-4 provided the best scar modification, and least damage to normal myocardium. During in vivo testing, CLG-4 application decreased BZ area (21.3±14.3mm² to 17.1±11.1 mm², p=0.043) and increased DS area (9.1±10.3 mm² to 22.0±20.6 mm², p=0.043). The total scar area before and after CLG application was 30.4±23.4mm² and 39.2±29.5 mm², respectively, p=0.08). LPs were reduced by CLG-4 application (28.8±21.8 to 13.8±13.1, p=0.043). During CLG-4 application (50.0±15.5 min), systolic blood pressure and heart rate were not significantly changed (68.0±7.7mmHg vs. 61.8±5.3mmHg, p=0.08; 77.4±7.3 beats per minute (BPM) vs. 78.8±6.0BPM, p=0.50, respectively).

Conclusions—Ventricular epicardial scar homogenization by CLG-4 application is feasible and effective. This represents the first report on bioenzymatic ablation of arrhythmogenic tissue as an alternative strategy for lesion formation.

Keywords

radiofrequency; ventricular tachycardia; collagenase; bioenzymatic ablation; scar homogenization

Address for correspondence: Kalyanam Shivkumar, MD, PhD, UCLA Cardiac Arrhythmia Center, UCLA Health System, David Geffen School of Medicine at UCLA, Suite 660, Westwood Blvd, Los Angeles CA 90095-1679, Tel: 310 206 6433, Fax: 310 794 6492, kshivkumar@mednet.ucla.edu.

Conflict of Interest Disclosures: The Regents of the University of California, Los Angeles has intellectual property developed by the author (KS) that relate to data reported in this paper.

Introduction

Catheter ablation is an established strategy for treating and preventing recurrent ventricular arrhythmias.^{1–3} A common approach to ventricular tachycardia (VT) ablation is targeting reentrant circuits through activation mapping and entrainment mapping, when the VT is hemodynamically tolerated.^{4, 5} VT episodes that result in hemodynamic instability are generally targeted by substrate modification during sinus rhythm. Electroanatomic mapping (EAM) helps delineate normal myocardial regions from abnormal ones, and identifies low-amplitude, delayed multicomponent electric activity, referred to as isolated late potentials (LPs). LPs may indicate areas of slow conduction that represent targets for catheter ablation of VT.^{6–8}

Radiofrequency (RF) energy delivery is most commonly used for catheter ablation,^{8, 9} however, alternative ablation energy sources such as cryoablation,^{10, 11} high-intensity focused ultrasound (HIFU),¹² laser^{13, 14} and microwave^{15, 16} have been studied. Chemical ablation by ethanol and coil embolization of a small coronary artery branch have also been reported.^{17, 18} The role of bioenzymatic agents in tissue homogenization of arrhythmic substrates, however, remains unknown.

Collagen subtypes I and III are abundant in myocardial scars^{19–22} and contribute to regions of slow conduction and electrical instability, known substrates for VT initiation.^{23, 24} Since border-zones (BZ) and LPs are characterized by surviving myocytes interspersed with scar,²⁵ we hypothesized that collagenase (CLG) application may induce focal digestion of both normal and scar tissue in BZs, thus homogenizing the scar and abolishing LPs in the process. The purpose of this study was to evaluate and characterize the feasibility of topical CLG application in homogenizing myocardial scars, and to assess the impact of CLG on LPs assessed by electro-anatomical mapping. We utilized a porcine infarct model, which closely resembles human myocardial scars. Optimal collagenase subtype and concentration were determined by in vitro experiments, and applied topically in vivo to epicardial scar regions.

Methods

Myocardial Infarct Induction

Myocardial infarcts (MI) were created in six female Yorkshire pigs (30 to 35 kg). Following a 12-hour fasting period, the animals were sedated with intramuscular injection of 1.4 mg/kg Telazol, and were intubated. Ventilation was achieved with an endotracheal tube connected to a ventilator (Summit Medical, Bend, OR). General anesthesia was maintained with inhaled 1.5% to 2.5% isoflurane. Analgesia was maintained with buprenorphine (0.3mg) intravenously hourly. Femoral arterial and venous access were obtained, and lidocaine (2.0mg/kg), esmolol (1.0mg/kg) and unfractionated heparin (10,000units) were given intravenously. Under fluoroscopic guidance, myocardial infarctions were created in the left circumflex (LCX) (n=1), right coronary (RCA) (n=2), and left anterior descending coronary arteries (LAD) (n=3). An Amplatz-type guide catheter was placed in the left main coronary artery or the RCA. A 0.018 mm guide wire (HT BMW Universal, Abbott vascular, IL) was inserted into the left coronary artery or the RCA. A 2.5–3.5 mm angioplasty balloon catheter (Fox sv, Abbott vascular, IL) was advanced over a guidewire and inflated in the mid-LCX/LAD or in the mid RCA. Thirty seconds after balloon inflation, a 10 mL suspension of sterile saline containing 3 to 5 mL polystyrene microspheres (Polybead® 90.0µm, Polysciences, PA) was injected through the central lumen of the balloon catheter. Electrocardiogram and arterial pressure were monitored continually during infarction and recovery. Acute infarction was confirmed by ST segment elevation in the electrocardiogram leads. Five minutes after microsphere injection, the balloon catheter was removed. Animals were extubated and observed with continuous electrocardiogram monitoring until able to

ambulate without assistance. Animals were observed without additional anti-arrhythmic drugs administered until terminal CLG-application experiments.

In Vitro Testing of Collagenase Subtypes

Three types of clostridial CLGs [Type 2 collagenase (CLG-2); Type 4 collagenase (CLG-4); and purified collagenase (CLSPA); Worthington Biochemical Corporation, NJ] were evaluated to identify the optimal CLG subtype, and concentration for scar homogenization.^{26–29} CLG-2, and CLG-4 were each tested at 6 concentrations (0.025%, 0.05%, 0.1%, 0.15%, 0.2% and 0.4%) while CLSPA was tested at 6 dilutions (25 U/mL, 50U/mL, 100 U/mL, 150 U/mL, 200 U/mL and 400 U/mL). The pieces of myocardium were obtained from a LCX infarct pig. The infarct was grossly evident on inspection, and was cut out into 20 equal pieces. The pieces of myocardium were subsequently histologically confirmed to contain scar, BZ and normal myocardium. A chemical buffer solution (HEPES, Sigma-Aldrich, MO) was used to dissolve each CLG subtype. The CLG solutions were adjusted to pH 7.4 – 7.5 for experimentation. Pieces of tissue soaked into HEPES medium served as controls. The solutions containing tissue were incubated at 37 °C for 24 hours. Histopathological analyses were performed to evaluate tissue digestion.

Collagenase Application In Vivo

Open chest surgery and topical application of CLG was performed in four animals. CLG-4 in 0.8% was used for each experiment. Cellulose sponge (small patch, 2×2 mm; large patch 3×5 cm; Cellulose sponge, Ningbo Kingyn, China) adsorbed with CLG-4 solution was placed onto the epicardial surface of the scar. The sponges were carefully placed within the low voltage areas where LPs were identified during EAM. The size of CLG-4 application area was decided based on the EAM results. During CLG application, the body was kept warm using a heating blanket. After confirming the feasibility of topical CLG application using the open chest approach, one additional animal was studied using a closed chest topical approach.³⁰ This involved devising a commercially available electrophysiologic ablation catheter, with a piece of cellulose sponge sutured tightly onto it (4mm SafireBLU, St. Jude Medical, MN). The facilitated visualization of the catheter on the EAM system, for precise delivery of CLG-4 to selected areas. After CLG-4 application in vivo, all animals (total n=5) subjected to CLG application were euthanized. Histopathological analyses were performed to evaluate scar homogenization.

Electroanatomic Mapping

Electroanatomic bipolar voltage mapping of epicardium was performed during sinus rhythm on the animals subjected to CLG application. The animals were heparinized during mapping and CLG application (3000 units unfractionated heparin intravenously every hour). The NavX patch system (EnSite, St. Jude Medical, MN) was used in the animal with closed-chest topical approach, while an EnSite array catheter system (EnSite, St. Jude Medical, MN) was used in the animals with open-chest approach. EnSite array was chosen to avoid the impact of air on impedance as assessed by NavX patch system. Data from both NavX patch and EnSite array systems were analyzed using NavX Velocity software (St. Jude Medical, MN). A duodecapolar catheter (Livewire, 2-2-2 mm spacing, St. Jude Medical, MN) and/or a 4 mm tip mapping catheter (SafireBLU, St. Jude Medical, MN) were used for epicardial mapping. During epicardial mapping, at least 500 points were collected for each pre- and post-CLG map.

All points on the interior projection >8 mm from the geometry (exterior projection for epicardial mapping) were considered to represent insufficient contact and excluded from the voltage map. Bipolar electrograms were band pass filtered between 30 and 300 Hz and displayed at a sweep speed of 100 mm/s. Three-dimensional bipolar electroanatomic maps

were displayed with dense scar (DS) defined as ≥ 0.5 mV, scar BZ from 0.51 to 1.50 mV, and total low-voltage area as ≥ 1.5 mV. Total low-voltage and DS areas were measured offline. Electrogram timing was measured manually during retrospective offline analysis. Late potential was defined as any low-voltage electrogram (≥ 1.5 mV) with a distinct onset after the QRS showing double or multiple components separated by a >20 msec isoelectric interval.³¹ Epicardial mapping was performed before and after CLG application. Total scar area, BZ area, DS area and the number of LPs (the number of mapped sites showing LPs) were quantified to compare between pre and post CLG application.

Histopathological Analysis

After euthanization, hearts were immediately explanted and rinsed thoroughly with cold saline 4°C. Subsequently cold 10% buffered formalin was flushed down the coronary arteries repeatedly. These samples were then placed in 10% buffered formalin for 24 to 48 hours, and then into 70% ethanol after rinsing in dH₂O. The sections were embedded in paraffin and cut in 5 micron-thick sections, and then stained with hematoxylin and eosin and trichrome-elastic van Gieson stains. Slides were digitally scanned for measurement of lesion depth (Aperio XT, Aperio Technologies, Vista, CA).

Statistical Analysis

The exact permutational version of the non-parametric Wilcoxon signed-rank test was used to compute *p* values for paired comparisons of hemodynamic data, total scar, dense scar, and border-zone areas before and after CLG application.

The exact non-parametric Mann-Whitney U test was used for unpaired comparisons of digestion depth. Data is displayed as dot plots. A *P* value of < 0.05 was considered significant. Analyses were performed with the use of SPSS version 19.0 statistical software (SPSS, Chicago, IL).

We verified catheter stability and reproducibility of local electrograms (including LPs) by sampling repeatedly at each location at different time intervals. Two observers analyzed the morphology and timing of these potentials. In cases in which a measurement or electrogram was subject to interpretation, a consensus between the two observers was reached.

Results

Determination of Optimal Collagenase Subtype

In vitro scar digestion was performed from adjacent blocks of myocardial tissue containing scar, BZ, and normal appearing myocardium. The procedural details are shown in Table 1. Three CLG subtypes were tested as previously described, CLG-2, CLG-4, and CLSPA. Concentrations tested were 0.025%, 0.05%, 0.1%, 0.15%, 0.2% and 0.4% for CLG-2 and CLG-4, and 25 U/mL, 50U/mL, 100 U/mL, 150 U/mL, 200 U/mL and 400 U/mL for CLPSA. Figure 1 shows histologic results from digestion experiments. Figure 1A shows control tissue block soaked in HEPES solution, while Figures 1E and 1I demonstrate high power views of the scar and normal appearing myocardium respectively from figure 1A. As shown in Figure 1B, 1F, and 1J, CLSPA (even at the highest concentration of 400U/ml), showed minimal digestion of the scar. However, the effects of CLG-2 (1C, 1G, and 1K) and CLG-4 (1D, 1H, and 1L) can be appreciated easily at doses of 0.4% for both CLG-2 and CLG-4. Below this dose, minimal digestion of scar or myocardium occurred (data not shown). The effect on scar digestion appeared greater in CLG-4 specimen than CLG-2, while the damage to surviving myocardium was stronger in specimen of CLG-2. The maximum depth of digestion of surviving myocardium was $665.9 \pm 58.3 \mu\text{m}$ for CLG-4 while that for CLG-2 was $951 \pm 39.6 \mu\text{m}$ ($p=0.01$) (Figure 1C and 1D; blue scale markers).

Impact of Collagenase on Scar and Border Zone Surface Area

In total, four animals underwent open-chest surgical approach (Figure 2A–2B), while one animal underwent a closed chest surgical approach using an ablation catheter with a piece of cellulose sponge fastened onto it (0.5cm by 1.0cm, figure 2C). This allowed the catheter to be directly visible within the EAM system and selectively placed over the BZ region (figure 2D). CLG-4 was applied on the RV epicardium for 30 min and LV epicardium for 60 min. In subject 5, CLG-4 was applied to three different sites for 30 min each (total 90 min) because of smaller sponge size. Mean CLG-4 application time was 60.0 ± 9.5 min across all animals, after which voltage mapping of the region was immediately repeated. The procedural details are shown in Table 2.

Hemodynamics were recorded continuously throughout the experiment. Systolic blood pressure and heart rate were not significantly changed before and after CLG application (68.0 ± 7.7 vs. 61.8 ± 5.3 mmHg, $p=0.08$; 77.4 ± 7.3 vs. 78.8 ± 6.0 beats/min, $p=0.50$, respectively).

Total low voltage and DS surface areas were measured in the NavX velocity system. Regions identified as border zones were targeted for digestion with CLG-4. The total scar area before and after application of CLG-4 was 30.4 ± 23.4 mm² and 39.2 ± 29.5 mm² respectively, ($p=0.08$, $n=5$). Topical application of CLG-4 significantly reduced BZ surface area (21.3 ± 14.3 mm² to 17.1 ± 11.1 mm², $p=0.043$, $n=5$) (Figure 3A). The reduction in BZ surface area was associated with an increase in DS surface area (9.1 ± 10.3 mm² to 22.0 ± 20.6 mm², $p=0.043$, $n=5$), indicating that CLG-4 application converted BZ areas to DS areas (Figure 3B). After CLG-4 delivery, the percentage of BZ was significantly reduced, while percent DS was significantly increased ($78.0 \pm 7.5\%$ to $53.0 \pm 9.7\%$, and $22.0 \pm 7.5\%$ to $47.0 \pm 9.7\%$, $p=0.043$, $n=5$; Figure 3C).

High-density mapping was performed in all animals, and LPs were quantified from all points collected. Consistent with previous studies³¹ the majority of LPs were distributed in the border zone. CLG-4 application significantly reduced the number of late potentials (28.8 ± 21.8 to 13.8 ± 13.1 , $p=0.043$, $n=5$) (figure 4). There was no significant difference in the total collected points pre- and post-CLG-4 application (704.5 ± 463.0 vs. 753.7 ± 438.0 , $p=0.14$).

Histopathological analyses were performed after CLG-4 application in all animals. Figures 5A and 5C show representative images of scar tissue after CLG-4 application in subjects 1 and 5, respectively. Focal debris and inflammatory changes were observed at CLG-4 application sites, while surviving myocardium distant from CLG-4 application sites remained intact. Extracellular matrix at CLG-4 application sites was degraded and appeared loosened (Figure 5B and D).

Discussion

Major Findings

The major findings of the present study are (i) collagenase application to the border zones results in chemical homogenization of myocardial scars and (ii) late potentials are eradicated after the collagenase application. The current study represents the first evaluation of bioenzymatic electrical scar homogenization.

Mechanism and Characteristics of Lesion Formation

The cardiac extracellular matrix (ECM) is surrounded by myocardium, and comprises several subtypes of collagens in normal hearts.³² Production of collagens induced by

myofibroblasts after myocardial infarction has been described in animal models and in humans. The BZ of scars, regions where myocardial scars are adjacent to surviving myocardium represent regions of slow conduction, and sources of VT. In this study, these regions were targeted for chemical ablation by CLG. The mechanism of lesion formation by CLG is the chemical interruption of tissue architecture given its inherent activity not only on collagens, but also its actions as a protease, an aminopeptidase, and a tryptase). This disruption involves both the normal and fibrotic components of the electrophysiologically defined BZ, rendering the region electrically silent. This causes not only mechanical but also electrical disconnection of surviving myocardium, and renders the BZ region electrical silent. These plural actions result in focal ablation of the cellular and ECM components of the targeted regions.

Ablation lesions created by RF energy delivery result in tissue coagulation necrosis, infiltration of inflammatory cells, and hemorrhage in central region, which ultimately form well-demarcated lesions. These lesions also results in obliteration of cellular and ECM components in normal myocardium and scar/BZ regions. Similarly, features of these ablation lesions are also observed in lesions created with HIFU, microwave and laser technology.³³ Biologic interruption of electrical conduction was reported by Bunch et al., where lesions were formed by fibroblast injection to modify atrioventricular node function.³⁴ That lesion was characterized by scar formation with collagen fibers. Others groups have performed delivery of biochemical solutions to myocardial scars by coronary artery injection or direct intramural injection.^{17, 34} Our study shows a novel method of epicardial scar digestion in the beating heart, involving catheters and devices already widely used clinically. Bioenzymatic ablation by CLG represents an alternate mechanism of lesion formation, which results in focal tissue destruction in regions exposed to the agent, similar to the aforementioned mechanical strategies. Topical application by open chest approach yielded focal delivery of collagenase and targeted digestion of the BZ regions only. We further showed feasibility of epicardial catheter-based delivery of CLG with focused effects on the BZ and on LPs.

Electrical Homogenization and Elimination of Late Potentials

The present study demonstrates electrical homogenization of myocardial scars, eliminating heterogeneous low voltage regions, and converting them into electrically silent DS. In addition, LPs, which predominantly exist in regions denoted as BZs, were significantly reduced after CLG application. Further, CLG application had no effects on LPs outside of the site of application. This is important as it indicates that the effects of CLG do not diffuse away and affect unintended sites. These findings suggest focal effects at regions exposed to CLG. Although arrhythmia inducibility was not tested, significant reduction in LPs suggests reduced tissue arrhythmogenicity. Clinical studies have shown that targeting and eradicating LPs is an effective strategy for catheter-based treatment of VT.^{31, 35} In the present study, CLG application was performed for 50 ± 15.5 min at a concentration of 0.8% for CLG-4. This application time can be dramatically shortened by increasing the concentration of CLG, making it more compatible for clinical use. A higher concentration of CLG can be applied at sites of interest, and the effects terminated by $\alpha 2$ -macroglobulin or other safe antagonists after a short period of time.

Study Limitations

This study demonstrates the feasibility of CLG in homogenizing myocardial scars and reducing LPs, as a proof of concept. A number of important considerations should be taken. Firstly, topical CLG application is more applicable for epicardial scars, although a percutaneous catheter providing a stable seal with the endocardium, excluding freely flowing blood could allow modulation of endocardial scars. Since we did not perform

endocardial voltage mapping, the effect of epicardial CLG application on the endocardium remains unknown. Hemodynamic measurements showed that CLG application did not cause hemodynamic compromise, although ventricular wall motion was not evaluated by echocardiography. Lastly, this study evaluated the effect of CLG application only in the acute phase, and the efficacy of lesion maintenance intermediate to long term remains unclear.

Conclusions

These data represent the first reported experimental evidence of the feasibility of bioenzymatic ablation of ventricular tissue. Further studies are warranted to investigate the safety and efficacy of this approach.

Acknowledgments

We are thankful to Dr. Jeffrey Gornbein of the UCLA Biostatistics core for assistance with this project.

Funding Sources: Supported by the NIH/NHLBI (National Heart Lung and Blood Institute) (R01HL084261 to KS)

References

1. Calkins H, Epstein A, Packer D, Arria AM, Hummel J, Gilligan DM, Trusso J, Carlson M, Luceri R, Kopelman H, Wilber D, Wharton JM, Stevenson W. Catheter ablation of ventricular tachycardia in patients with structural heart disease using cooled radiofrequency energy: Results of a prospective multicenter study. Cooled RF multi center investigators group. *J Am Coll Cardiol.* 2000; 35:1905–1914. [PubMed: 10841242]
2. Kuck KH, Schaumann A, Eckardt L, Willems S, Ventura R, Delacretaz E, Pitschner HF, Kautzner J, Schumacher B, Hansen PS. group Vs. Catheter ablation of stable ventricular tachycardia before defibrillator implantation in patients with coronary heart disease (VTACH): A multicentre randomised controlled trial. *Lancet.* 2010; 375:31–40. [PubMed: 20109864]
3. Stevenson WG, Wilber DJ, Natale A, Jackman WM, Marchlinski FE, Talbert T, Gonzalez MD, Worley SJ, Daoud EG, Hwang C, Schuger C, Bump TE, Jazayeri M, Tomassoni GF, Kopelman HA, Soejima K, Nakagawa H. Multicenter Thermocool VTATI. Irrigated radiofrequency catheter ablation guided by electroanatomic mapping for recurrent ventricular tachycardia after myocardial infarction: The multicenter thermocool ventricular tachycardia ablation trial. *Circulation.* 2008; 118:2773–2782. [PubMed: 19064682]
4. de Bakker JM, van Capelle FJ, Janse MJ, Wilde AA, Coronel R, Becker AE, Dingemans KP, van Hemel NM, Hauer RN. Reentry as a cause of ventricular tachycardia in patients with chronic ischemic heart disease: Electrophysiologic and anatomic correlation. *Circulation.* 1988; 77:589–606. [PubMed: 3342490]
5. Stevenson WG, Khan H, Sager P, Saxon LA, Middlekauff HR, Natterson PD, Wiener I. Identification of reentry circuit sites during catheter mapping and radiofrequency ablation of ventricular tachycardia late after myocardial infarction. *Circulation.* 1993; 88:1647–1670. [PubMed: 8403311]
6. Marchlinski FE, Callans DJ, Gottlieb CD, Zado E. Linear ablation lesions for control of unmappable ventricular tachycardia in patients with ischemic and nonischemic cardiomyopathy. *Circulation.* 2000; 101:1288–1296. [PubMed: 10725289]
7. Soejima K, Suzuki M, Maisel WH, Brunckhorst CB, Delacretaz E, Blier L, Tung S, Khan H, Stevenson WG. Catheter ablation in patients with multiple and unstable ventricular tachycardias after myocardial infarction: Short ablation lines guided by reentry circuit isthmuses and sinus rhythm mapping. *Circulation.* 2001; 104:664–669. [PubMed: 11489772]
8. Cesario DA, Mahajan A, Shivkumar K. Lesion-forming technologies for catheter ablation of atrial fibrillation. *Heart Rhythm.* 2007; 4:S44–50. [PubMed: 17336884]
9. Nakagawa H, Yamanashi WS, Pitha JV, Arruda M, Wang X, Ohtomo K, Beckman KJ, McClelland JH, Lazzara R, Jackman WM. Comparison of in vivo tissue temperature profile and lesion geometry

for radiofrequency ablation with a saline-irrigated electrode versus temperature control in a canine thigh muscle preparation. *Circulation*. 1995; 91:2264–2273. [PubMed: 7697856]

10. Deisenhofer I, Zrenner B, Yin YH, Pitschner HF, Kuniss M, Grossmann G, Stiller S, Luik A, Veltmann C, Frank J, Linner J, Estner HL, Pflaumer A, Wu J, von Bary C, Ucer E, Reents T, Tzeis S, Fichtner S, Kathan S, Karch MR, Jilek C, Ammar S, Kolb C, Liu ZC, Haller B, Schmitt C, Hessling G. Cryoablation versus radiofrequency energy for the ablation of atrioventricular nodal reentrant tachycardia (the cyrano study): Results from a large multicenter prospective randomized trial. *Circulation*. 2010; 122:2239–2245. [PubMed: 21098435]
11. Skanes AC, Dubuc M, Klein GJ, Thibault B, Krahn AD, Yee R, Roy D, Guerra P, Talajic M. Cryothermal ablation of the slow pathway for the elimination of atrioventricular nodal reentrant tachycardia. *Circulation*. 2000; 102:2856–2860. [PubMed: 11104744]
12. Strickberger SA, Tokano T, Kluiwstra JU, Morady F, Cain C. Extracardiac ablation of the canine atrioventricular junction by use of high-intensity focused ultrasound. *Circulation*. 1999; 100:203–208. [PubMed: 10402451]
13. Pfeiffer D, Moosdorf R, Svenson RH, Littmann L, Grimm W, Kirchhoff PG, Luderitz B. Epicardial neodymium. Yag laser photocoagulation of ventricular tachycardia without ventriculotomy in patients after myocardial infarction. *Circulation*. 1996; 94:3221–3225. [PubMed: 8989132]
14. Ware DL, Boor P, Yang C, Gowda A, Grady JJ, Motamedi M. Slow intramural heating with diffused laser light: A unique method for deep myocardial coagulation. *Circulation*. 1999; 99:1630–1636. [PubMed: 10096942]
15. Thomas SP, Clout R, Deery C, Mohan AS, Ross DL. Microwave ablation of myocardial tissue: The effect of element design, tissue coupling, blood flow, power, and duration of exposure on lesion size. *J Cardiovasc Electrophysiol*. 1999; 10:72–78. [PubMed: 9930912]
16. Wayne JG, Nath S, Haines DE. Microwave catheter ablation of myocardium in vitro. Assessment of the characteristics of tissue heating and injury. *Circulation*. 1994; 89:2390–2395. [PubMed: 8181165]
17. Brugada P, de Swart H, Smeets JL, Wellens HJ. Transcoronary chemical ablation of ventricular tachycardia. *Circulation*. 1989; 79:475–482. [PubMed: 2917386]
18. Tholakanahalli VN, Bertog S, Roukoz H, Shivkumar K. Catheter ablation of ventricular tachycardia using intracoronary wire mapping and coil embolization: Description of a new technique. *Heart Rhythm*. 2013; 10:292–296. [PubMed: 23089899]
19. Luther DJ, Thodeti CK, Shamhart PE, Adapala RK, Hodnichak C, Weihrauch D, Bonaldo P, Chilian WM, Meszaros JG. Absence of type vi collagen paradoxically improves cardiac function, structure, and remodeling after myocardial infarction. *Circ Res*. 2012; 110:851–856. [PubMed: 22343710]
20. Cleutjens JP, Verluyten MJ, Smiths JF, Daemen MJ. Collagen remodeling after myocardial infarction in the rat heart. *Am J pathol*. 1995; 147:325–338. [PubMed: 7639329]
21. Lopez B, Gonzalez A, Diez J. Circulating biomarkers of collagen metabolism in cardiac diseases. *Circulation*. 2010; 121:1645–1654. [PubMed: 20385961]
22. Uusimaa P, Risteli J, Niemela M, Lumme J, Ikaheimo M, Jounela A, Peuhkurinen K. Collagen scar formation after acute myocardial infarction: Relationships to infarct size, left ventricular function, and coronary artery patency. *Circulation*. 1997; 96:2565–2572. [PubMed: 9355895]
23. Rutherford SL, Trew ML, Sands GB, LeGrice IJ, Smaill BH. High-resolution 3-dimensional reconstruction of the infarct border zone: Impact of structural remodeling on electrical activation. *Circ Res*. 2012; 111:301–311. [PubMed: 22715470]
24. Ursell PC, Gardner PI, Albala A, Fenoglio JJ Jr, Wit AL. Structural and electrophysiological changes in the epicardial border zone of canine myocardial infarcts during infarct healing. *Circ Res*. 1985; 56:436–451. [PubMed: 3971515]
25. Nakahara S, Tung R, Ramirez RJ, Gima J, Wiener I, Mahajan A, Boyle NG, Shivkumar K. Distribution of late potentials within infarct scars assessed by ultra high-density mapping. *Heart Rhythm*. 2010; 7:1817–1824. [PubMed: 20682358]

26. Hoppe UC, Jansen E, Sudkamp M, Beuckelmann DJ. Hyperpolarization-activated inward current in ventricular myocytes from normal and failing human hearts. *Circulation*. 1998; 97:55–65. [PubMed: 9443432]
27. Masson-Pevet M, Jongasma HJ, De Bruijne J. Collagenase- and trypsin-dissociated heart cells: A comparative ultrastructural study. *J Mol Cell Cardiol*. 1976; 8:747–757. [PubMed: 186609]
28. Todor A, Sharov VG, Tanhehco EJ, Silverman N, Bernabei A, Sabbah HN. Hypoxia-induced cleavage of caspase-3 and dff45/icad in human failed cardiomyocytes. *Am J Physiol Heart Circ Physiol*. 2002; 283:H990–995. [PubMed: 12181128]
29. Zhou YY, Wang SQ, Zhu WZ, Chruscinski A, Kobilka BK, Ziman B, Wang S, Lakatta EG, Cheng H, Xiao RP. Culture and adenoviral infection of adult mouse cardiac myocytes: Methods for cellular genetic physiology. *Am J Physiol Heart Circ Physiol*. 2000; 279:H429–436. [PubMed: 10899083]
30. Sosa E, Scanavacca M, d'Avila A, Pilleggi F. A new technique to perform epicardial mapping in the electrophysiology laboratory. *J Cardiovasc Electrophysiol*. 1996; 7:531–536. [PubMed: 8743758]
31. Nakahara S, Tung R, Ramirez RJ, Michowitz Y, Vaseghi M, Buch E, Gima J, Wiener I, Mahajan A, Boyle NG, Shivkumar K. Characterization of the arrhythmogenic substrate in ischemic and nonischemic cardiomyopathy implications for catheter ablation of hemodynamically unstable ventricular tachycardia. *J Am Coll Cardiol*. 2010; 55:2355–2365. [PubMed: 20488307]
32. Bishop JE, Laurent GJ. Collagen turnover and its regulation in the normal and hypertrophying heart. *Eur Heart J*. 1995; 16 (Suppl C):38–44. [PubMed: 7556271]
33. Haines DE, Verow AF, Sinusas AJ, Whayne JG, DiMarco JP. Intracoronary ethanol ablation in swine: Characterization of myocardial injury in target and remote vascular beds. *J Cardiovasc Electrophysiol*. 1994; 5:41–49. [PubMed: 8186876]
34. Bunch TJ, Mahapatra S, Bruce GK, Johnson SB, Miller DV, Horne BD, Wang XL, Lee HC, Caplice NM, Packer DL. Impact of transforming growth factor-beta1 on atrioventricular node conduction modification by injected autologous fibroblasts in the canine heart. *Circulation*. 2006; 113:2485–2494. [PubMed: 16717152]
35. Di Biase L, Santangeli P, Burkhardt DJ, Bai R, Mohanty P, Carbucicchio C, Dello Russo A, Casella M, Mohanty S, Pump A, Hongo R, Beheiry S, Pelargonio G, Santarelli P, Zucchetti M, Horton R, Sanchez JE, Elayi CS, Lakkireddy D, Tondo C, Natale A. Endo-epicardial homogenization of the scar versus limited substrate ablation for the treatment of electrical storms in patients with ischemic cardiomyopathy. *J Am Coll Cardiol*. 2012; 60:132–141. [PubMed: 22766340]

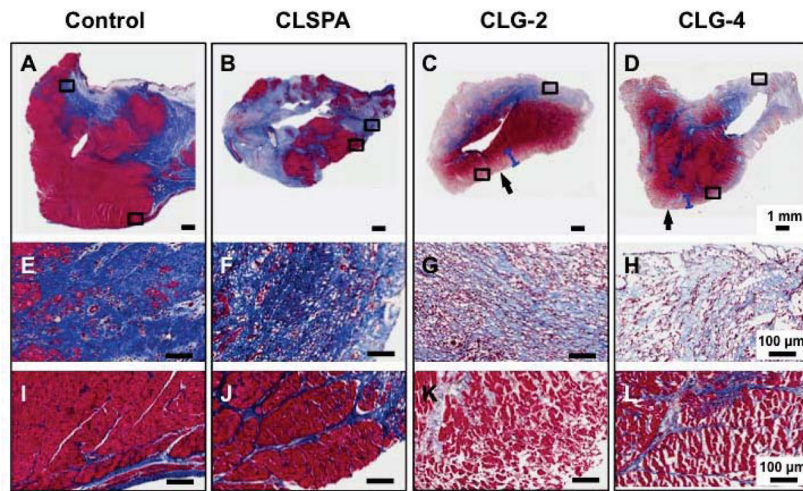


Figure 1. Collagenase application in vitro: Shown are trichrome elastic von Giessen images of tissue soaked into (A) HEPES (control), (B) Purified collagenase (CLSPA) solution (400 U/mL), (C) collagenase type 2 (CLG-2) 0.4% and (D) collagenase type 4 (CLG-4) 0.4% (Scale bar, 1 mm). Scar tissue is stained blue. (E) to (H) indicate corresponding higher-power fields of collagenous fibrotic scar area from (A) to (D) respectively, and adjacent myocardium in (I) to (L) respectively (magnification $\times 10$; scale bar, 100 μm). Arrows indicate regions digested, and blue scale bars indicate depth of myocardial digestion.

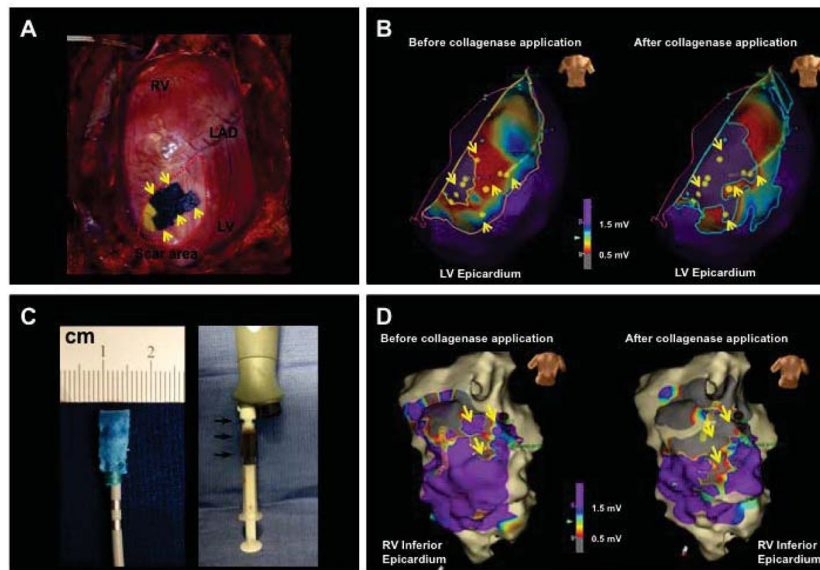


Figure 2. Collagenase delivery strategies: **A**, Image of collagenase type 4 (CLG-4) application in subject 3 using small cellulose sponges (2×2 mm). **B**, Bipolar voltage map before and after CLG-4 application in subject 3. Yellow arrows indicate CLG-4 application site. **C**, Cellulose sponge (0.5×1 cm) tied to the tip of an irrigation catheter. Black arrows indicate CLG-4 solution connected to irrigation lumen. **D**, Bipolar voltage map of right ventricular inferior epicardium before and after CLG-4 application in subject 5. Dense scar lesion with voltage < 0.5 mV is shown in gray. Yellow arrows indicate CLG-4 application site.

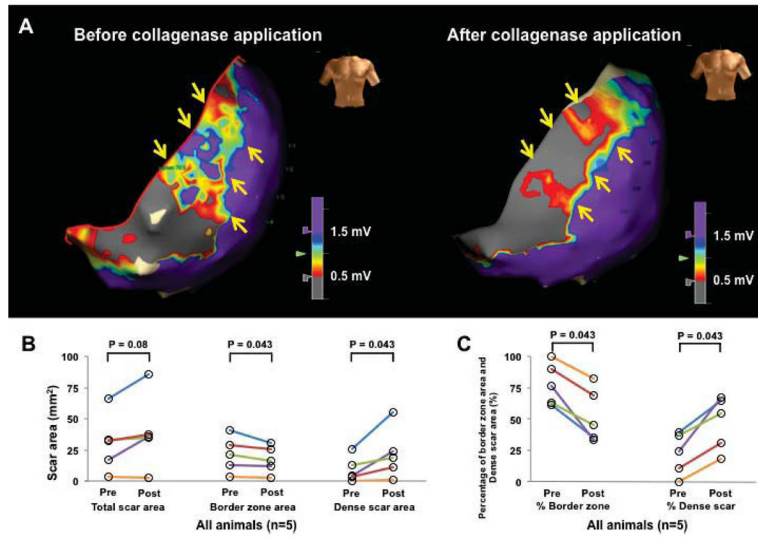


Figure 3. Change in low voltage area after collagenase application: **A**, Bipolar voltage map before and after collagenase type 4 (CLG-4) application. Dense scar lesion with voltage < 0.5 mV was delineated in gray areas. Yellow arrows indicate CLG-4 application site. **B**, Quantification of scar area in the animals with CLG-4 selectively applied (n = 5). **C**, Quantification of border zone and dense scar distribution in scar area.

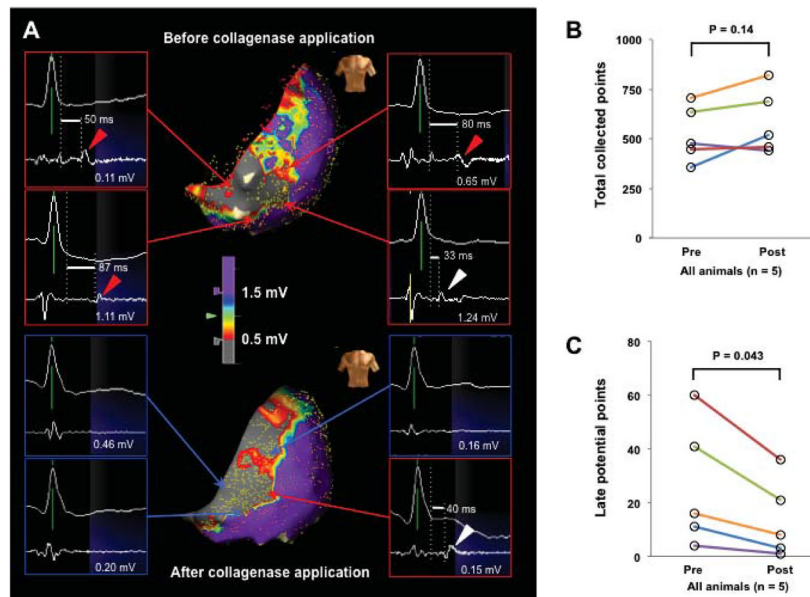


Figure 4. Collagenase application eliminates late potentials: **A**, Bipolar voltage map and isolated late potential (LP) distribution before and after collagenase type 4 (CLG-4) application. Red arrows indicate LPs in the scar area, and red arrowheads indicate actual LPs on the electrogram. Blue arrows indicate LP eliminated points. **B**, Quantification of total collected points from electro-anatomical maps before and after CLG-4 application. **C**, Quantification of the number of LPs before and after CLG-4 application. The white arrows denote a LP that remained after CLG-4 application.

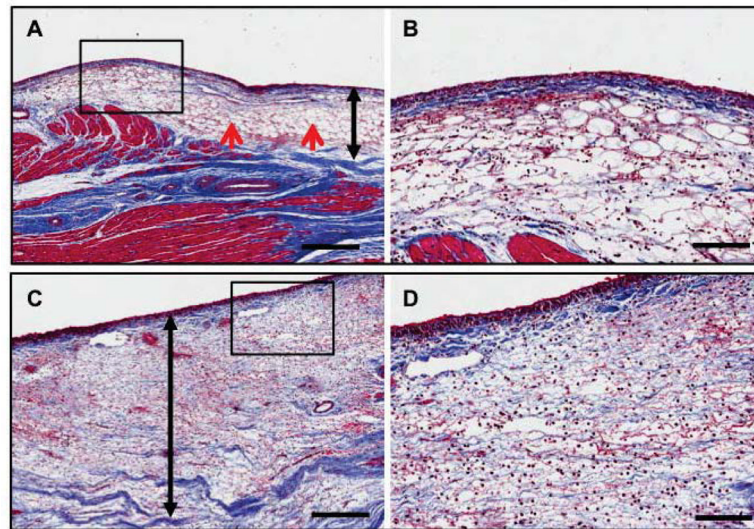


Figure 5. Histopathological analyses after collagenase application: Representative images of trichrome elastic von Giessen staining of scar tissue after collagenase type 4 (CLG-4) application in (A) subject 1 and (C) subject 5 (scale bar, 250 μm). (B) and (D) indicate corresponding higher-power fields of (A) and (C), respectively (scale bar 100 μm). Red arrows indicate connective tissue loosening. Black double-sided arrows indicate the approximate range of digestion lesion.

Table 1

Procedural details of in vitro experiments

Collagenase subtype	Maximum concentration	Application time (hours)	Digestion depth (μm)
Control	n/a	24	0
CLSPA	400 (U/mL)	24	0
CLG-2	0.4 (%)	24	665.9 \pm 58.3
CLG-4	0.4 (%)	24	951.0 \pm 39.6*

Values for digestion depth are listed as mean \pm SEM.

CLSPA = Purified collagenase; CLG-2 = Collagenase type 2; CLG-4 = Collagenase type 4.

* $P < 0.05$ when compared to CLG-2.

Table 2

Procedural details of collagenase application strategies

Subject	Infarcted artery	Time from infarction to ablation (Days)	Weight (kg)	Epicardial access	Electroanatomic mapping system	Mapping area	Application strategy	Application time (min)	Lesion depth (mm)
1	RCA	58	55.3	Open Chest	EnSite array NavX Velocity	RV Epi	Large cellulose sponge	30	1.43
2	LAD	34	40.4	Open Chest	EnSite array NavX Velocity	LV Epi	Small cellulose sponge	60	2.10
3	LAD	40	40.4	Open Chest	EnSite array NavX Velocity	LV Epi	Small cellulose sponge	60	1.84
4	LAD	49	43.5	Open Chest	EnSite array NavX Velocity	LV Epi	Small cellulose sponge	60	1.30
5	RCA	52	53.7	Closed-chest percutaneous puncture	NavX patch NavX Velocity	RV Inferior Epi	Cellulose sponge catheter	90	1.50
Average ± SEM		46.6 ± 4.3	46.7 ± 3.3					60.0 ± 9.5	1.63 ± 0.15

RCA = right coronary artery; LAD = left anterior descending artery; RV = right ventricle; LV = left ventricle; Epi = epicardium. kg = kilogram; min = minute; mm = millimeter.